A Partial Variational Analysis of Planar Dielectric Antennas

Shyh-Jong Chung and Chun Hsiung Chen, *Senior Member, IEEE*

***Abstract*—The reflection and radiation characteristics of a planar dielectric antenna with arbitrary geometrical configuration are analyzed numerically. A variational equation is first established based on the partial variational principle (PVP), and then solved by the finite element method coupled with the frontal solution technique. The radiation and boundary conditions are incorporated by combining the modal expansion method and the Green's function approach for exterior field representation. The reflection coefficients, the radiation patterns, and the directive and power gains of several antennas with linearized structures are studied and compared.**

I. Introduction

DIELECTRIC antennas are essential parts of millimeter- and submillimeter-wave systems. Owing to the complexity of the problem, many authors have paid attention to the elementary problem of planar structure rather than rod structure in obtaining a simplified picture for radiation mechanism. Angulo [1] first derived a variational formulation for the terminal impedance of a semi-infinite dielectric slab structure, and then used the incident surface wave as a trial field. Butler and Zoroofchi [2] took the Fourier transform of the incident field, and summed up the reflected and refracted fields of all spectral components to get the total reflected and transmitted waves. Ikegami [3] solved a matrix equation for the reflection coefficients by neglecting the continuous spectrum in a dielectric slab guide.

Various approximation techniques were developed to find the far-field pattern of a semi-infinite planar dielectric structure [4]–[7], among which Lewin [7] derived a spectral integral equation and gave a theoretical comparison of these approximation techniques. Without approximation, Gelin *et al.* [8] solved the spectral integral equation numerically by iteration via the Neumann series.

In a different approach, Rozzi *et al.* [9] solved a field integral equation by the Ritz–Galerkin method. Here, the normalized Lagurre polynomials were used both to expand the junction fields and to weight the integral equation. By using the free-space Green's function coupled with geometrical optics, Nishimura *et al.* [10] tackled a field integral equation by iteration. Recently, Capsalis *et al.* [11] iteratively solved a Fredholm integral equation of the second kind without making approximations on the waveguide Green's function.

Manuscript received May 26, 1988; revised January 2, 1991. This work was supported by the National Science Council, Republic of China, under Grant NSC 77-0404-E002-01.

S.-J. Chung is with the Department of Communication Engineering, National Chiao Tung University, Hsinchu, Taiwan, Republic of China.

C. H. Chen is with the Department of Electrical Engineering, National Taiwan University, Taipei, Taiwan, Republic of China.

IEEE Log Number 9100279.

The previous methods can efficiently or rigorously treat the abruptly terminated planar dielectric structure, while none of them, except [10], can handle the arbitrarily shaped one. In this investigation, the partial variational approach [12], [13] will be adopted to deal with the planar dielectric antenna with arbitrary shape and refractive index. A variational equation is first derived by following the concept of the partial variational principle (PVP) [12], and is then solved by the finite element method together with the frontal solution technique [14]. The exterior fields involved in the variational equation are tackled by the modal expansion method linked with the Green's function approach [13]. Numerical results are obtained and compared with those of other methods. Finally included are the reflection coefficients and far-field patterns for various antenna structures.

II. Variational Formulation

Consider a planar dielectric antenna structure shown in Fig. 1(a), which is uniform in the y direction and symmetric with respect to the y-z plane. For excitation, the arbitrarily shaped dielectric antenna of refractive index $n(x, z)$ is connected to a planar dielectric waveguide of refractive index n_1 and width $2t$. Suppose that even TE guided modes are incident upon the dielectric antenna, then some power will be reflected back to the waveguide in the form of guided modes, and the other will radiate into the surrounding free space. For theoretical analysis, the structure may be replaced by the half structure shown in Fig. 1(b), where an infinite magnetic wall Γ_0 is introduced by symmetry. The whole space is divided into four regions, that is, the finite element region $\Omega(0 \le x \le X_0, 0 \le z \le l)$, the waveguide region I $(0 \le x < \infty, -\infty < z \le 0)$, the first free-space region II $(0 \le x < \infty, l \le z < \infty)$, and the second free-space region III $(X_0 \le x < \infty, -\infty < z < \infty)$. Note that regions I and III as well as II and III are overlapped in Fig. 1(b).

Before the derivation of the partial variational equation, a general description may be needed. The fields introduced to simulate the exact ones, (which are named "trial fields" in the following), may be divided into two groups, that is, those inside Ω and outside Ω. For the trial fields inside Ω, one may choose the electric field as unknown variables and express the magnetic field in functions of the electric field. In doing so, a residual electric volume source may arise to support the trial fields. For the trial fields outside Ω, we choose those that satisfy source-free Maxwell's equations, the radiation condition, and all the boundary conditions except that on the boundary $\Gamma(= \Gamma_1 + \Gamma_2 + \Gamma_3)$. (In fact, this is the most difficult portion of this approach and is handled in Section III.) These two groups of trial fields in general may introduce

0018-926X/91/0600-0713$01.00

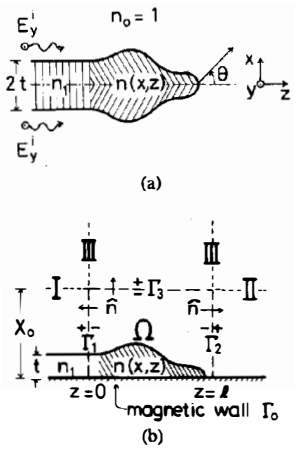

Fig. 1. (a) Geometry of planar dielectric antenna. (b) Reduced structure for analysis.

surface currents at Γ. Now since the problem is source free in the entire region, the electric volume current in Ω and the surface currents at Γ should be weighted to zero so that the trial fields may become the exact ones.

Let $\bar{E}(\Omega)$ be the trial electric field inside Ω with the corresponding magnetic field $\bar{H}(\Omega)$ given by

$$\bar{H}(\Omega) = \frac{j}{\omega\mu_0}\nabla \times \bar{E}(\Omega). \tag{1}$$

For this arbitrarily chosen $\bar{E}(\Omega)$, there must be a supporting volume electric current $\bar{J}$ inside Ω

$$\bar{J}(\Omega) = \nabla \times \bar{H}(\Omega) - j\omega\epsilon\bar{E}(\Omega) \tag{2}$$

where $\epsilon(x, z) = n^2(x, z)\epsilon_0$ is the permittivity in Ω and $\bar{H}(\Omega)$ is a function of $\bar{E}(\Omega)$ by (1).

The trial fields $(\bar{E}, \bar{H})$ outside Ω are chosen independently so as to satisfy the source-free Maxwell's equations and the boundary condition on the magnetic wall Γ_0 $(-\infty < z \le 0; l \le z < \infty)$. Associated with these two independent field sets, inside and outside Ω, are the surface electric current $(\bar{K})$ and magnetic current $(\bar{N})$ over the boundary Γ,

$$\bar{K}(\Gamma) = \hat{n} \times \left[\bar{H}(\Gamma^+) - \bar{H}(\Gamma^-)\right] \tag{3}$$

$$\bar{N}(\Gamma) = -\hat{n} \times \left[\bar{E}(\Gamma^+) - \bar{E}(\Gamma^-)\right] \tag{4}$$

so that the continuity boundary conditions over Γ may be incorporated. Here, $\Gamma = \Gamma_1 + \Gamma_2 + \Gamma_3$ and $\hat{n}$ denotes the outward normal of the boundary Γ whose inner and outer sides are represented by Γ^- and Γ^+, respectively. In addition, the trial fields $(\bar{E}(\Omega), \bar{H}(\Omega))$ inside Ω should also be supported by the surface currents over the magnetic wall $\Gamma_0(0 \le z \le l)$ (denoted by Γ_{00})

$$\bar{K}(\Gamma_{00}) = -\hat{n} \times \bar{H}(\Gamma_{00}^-) \tag{5}$$

$$\bar{N}(\Gamma_{00}) = \hat{n} \times \bar{E}(\Gamma_{00}^-), \tag{6}$$

here $\hat{n} = -\hat{x}$.

Since the problem is source free, the volume current $\bar{J}(\Omega)$ in (2) and the surface currents $\bar{K}(\Gamma)$, $\bar{N}(\Gamma)$, and $\bar{K}(\Gamma_{00})$ in (3), (4), and (5) should be zero for the true fields so that the following equation holds for arbitrary variation fields $(\delta^a\bar{E}^a, \delta^a\bar{H}^a)$:

$$\begin{aligned}\int_\Omega dv\,\delta^a\bar{E}^a(\Omega) \cdot \bar{J}(\Omega) &+ \int_\Gamma ds\left[\delta^a\bar{E}^a(\Gamma^-) \cdot \bar{K}(\Gamma) - \delta^a\bar{H}^a(\Gamma^+) \cdot \bar{N}(\Gamma)\right] \\ &+ \int_{\Gamma_{00}} ds\,\delta^a\bar{E}^a(\Gamma_{00}^-) \cdot \bar{K}(\Gamma_{00}) \\ &= 0.\end{aligned} \tag{7}$$

Here δ^a is a variational operator which operates only on the fields with superscript a [12] and $(\bar{E}^a, \bar{H}^a)$ are fields independent of $(\bar{E}, \bar{H})$.

By removing the operator δ^a outside of the integrals of (7) and substituting the supporting sources by (2)–(5) and the magnetic field inside Ω by (1), one then obtains the following variational equation:

$$\begin{aligned}&\delta^a I^a = 0 \\ &I^a = \frac{j}{\omega\mu_0}\int_\Omega dv\left[\frac{\partial E_y^a}{\partial x}\frac{\partial E_y}{\partial x} + \frac{\partial E_y^a}{\partial z}\frac{\partial E_y}{\partial z} - k_0^2 n^2 E_y^a E_y\right] \\ &\quad + \int_\Gamma ds\,\hat{n} \cdot \left[\hat{z}H_x^a(\Gamma^+) - \hat{x}H_z^a(\Gamma^+)\right] \\ &\quad \cdot \left[E_y(\Gamma^-) - E_y(\Gamma^+)\right] \\ &\quad - \int_\Gamma ds\,E_y^a(\Gamma^-)\hat{n} \cdot \left[\hat{x}H_z(\Gamma^+) - \hat{z}H_x(\Gamma^+)\right]\end{aligned} \tag{8}$$

where $k_0 = \omega\sqrt{\mu_0\epsilon_0}$ is the propagation constant of free space. Note that $(\bar{E}, \bar{H}) = (E_y; H_x, H_z)$ and $(\bar{E}^a, \bar{H}^a) = (E_y^a; H_x^a, H_z^a)$ are incorporated in (7) and that integration by part has been used in the volume integral to reduce the order of the derivative with respect to E_y. Also note that the surface integral on Γ_{00} in (7) is canceled by that obtained after the process of integration by part.

III. Finite Element Approach and Exterior Field Representations

Equation (8) is solved by the finite element method [14]. The region Ω is divided into several numbered triangular elements as shown in Fig. 2, each with six nodes (3 on the vertices and 3 on the mid-points of the sides). The field E_y^e at the eth element is expanded by the nodal field value ϕ_i^e (unknown) and the shape function N_i [14]:

$$E_y^e(x, z) = \sum_{i=1}^{6} \phi_i^e N_i. \tag{9}$$

Here N_i's are second-order polynomial functions of x and z. Specifically

$$N_i(x, z) = \delta_{ij}, \qquad \text{for } (x, z) = (x_j, z_j)$$

with (x_j, z_j) being the coordinate of the jth node and δ_{ij} the Kronecker delta.

The unknown variables associated with the surface integral on Γ are all arranged as the boundary element (the last element). These include the electric field just interior to Γ

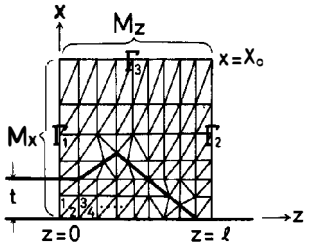

Fig. 2. Typical finite element mesh division with second-order triangular elements.

and the electric and magnetic fields just exterior to Γ (see (8)). The former is represented by the nodal values and shape functions as (9). The latter, which should satisfy the source-free Maxwell's equations and all boundary conditions (except on Γ), is classified into two parts, that is, the fields in waveguide I and free space II (those for Γ_1 and Γ_2, respectively) and the fields in free space III (those for Γ_3).

A. Fields in Waveguide I and Free Space II

The fields in region I are expanded by the discrete guided modes and continuous radiation modes of the slab waveguide, while in region II no guided mode exists and the fields are expanded only by the sinusoidal functions of continuous spectrum (ρ):

$$E_y^\alpha(x,z) = s_\alpha\left\{\sum_{m=1}^{N_1}\left[A_m e^{-j\beta_m z} + a_m e^{j\beta_m z}\right]u_m(x)\right\} + \int_0^\infty d\rho\, d_\rho^\alpha \frac{\omega\mu_0}{\beta_\rho} u_\rho^\alpha(x) e^{\pm j\beta_\rho(z-z_\alpha)} \tag{10}$$

$$\omega\mu_0 H_x^\alpha(x,z) = s_\alpha\left\{\sum_{m=1}^{N_1}\beta_m\left[-A_m e^{-j\beta_m z} + a_m e^{j\beta_m z}\right]u_m(x)\right\} \pm \omega\mu_0\int_0^\infty d\rho\, d_\rho^\alpha u_\rho^\alpha(x) e^{\pm\beta_\rho(z-z_\alpha)}. \tag{11}$$

For the waveguide region, $\alpha = \mathrm{I}$, $s_\alpha = 1$, $z_\alpha = 0$, and the upper signs are used. For the free-space region, $\alpha = \mathrm{II}$, $s_\alpha = 0$ (no discrete modes), $z_\alpha = \ell$, and the lower signs are used. N_1 is the number of discrete guided modes in the slab waveguide. A_m and a_m are the coefficients for the incident (known) and scattered (unknown) guided modes (discrete spectrum) with modal function and propagation constant denoted by $u_m(x)$ and β_m. $u_\rho^\alpha(x)$ and d_ρ^α (unknown) are the modal function (which is sinusoidal function for free space II) and the coefficient of the radiation mode (continuous spectrum) in region α, where ρ and $\beta_\rho = \sqrt{k_1^2 - \rho^2}$ are the wavenumbers in the x- and z-directions, respectively.

The field representations (10) and (11) are not suitable for numerical computation since the unknown d_ρ's are the continuous functions of ρ. It is necessary to change the representations into other forms with discrete unknown variables.

The modal functions are expanded, using the normalized Lagurre polynomials $\{\mathcal{L}_q(x)\}$ [15]:

$$u_m(x) = \sum_{q=1}^{M} Q_{mq}\mathcal{L}_q(x) \tag{12}$$

$$u_\rho^\alpha(x) = \sum_{q=1}^{M} P_{\rho q}^\alpha \mathcal{L}_q(x) \tag{13}$$

where M is a finite number and

$$Q_{mq} = \int_0^\infty dx\, u_m(x)\,\mathcal{L}_q(x) \tag{14}$$

$$P_{\rho q}^\alpha = \int_0^\infty dx\, u_\rho^\alpha(x)\,\mathcal{L}_q(x) \tag{15}$$

The desired complete and orthonormal set $\{\mathcal{L}_q(x)\}$ in $0 \le x < \infty$ is defined by

$$\mathcal{L}_q(x) = \frac{1}{\sqrt{S_0}}\exp(-x/2S_0)L_{q-1}\left(\frac{x}{S_0}\right), \quad q = 1,2,\cdots \tag{16}$$

where L denotes the Lagurre polynomial. The suitable scale factor S_0 is chosen based on the criterion that (12) can essentially be satisfied for a given M [15], and that the sequence of (16) is numerically independent in $0 \le x \le X_0$.

Now expand the magnetic fields at $z = z_\alpha$ ($= 0$ or ℓ) as

$$\omega\mu_0 H_x(\Gamma_\alpha^+) = \omega\mu_0 H_x^\alpha(x, z_\alpha) = -s_\alpha\sum_{m=1}^{N_1}\beta_m A_m u_m(x) + \sum_{q=1}^{M} h_q^\alpha \mathcal{L}_q(x) \tag{17}$$

where h_q's are to be determined.

Equating (17) and (11) at $z = z_\alpha$, then using the modal orthogonality property and (14) and (15), one finds

$$a_m = \sum_{q=1}^{M} h_q^I\left(\frac{Q_{mq}}{\beta_m}\right) \tag{18}$$

$$d_\rho^\alpha = \pm\sum_{q=1}^{M} h_q^\alpha\left(\frac{P_{\rho q}^\alpha}{\omega_{\mu 0}}\right). \tag{19}$$

Substituting (18), (19), (12), and (13) into (10) gives

$$E_y(\Gamma_\alpha^+) = E_y^\alpha(x, z_\alpha) = s_\alpha\sum_{m=1}^{N_1} A_m u_m(x) \pm \sum_{q=1}^{M} h_q^\alpha\left[\sum_{p=1}^{M} Z_{qp}^\alpha \mathcal{L}_p(x)\right] \tag{20}$$

where

$$Z_{qp}^\alpha = s_\alpha\sum_{m=1}^{N_1}\frac{1}{\beta_m}Q_{mq}Q_{mp} + \int_0^\infty d\rho\frac{P_{\rho q}^\alpha P_{\rho p}^\alpha}{\beta_\rho}. \tag{21}$$

The exterior tangential fields over the boundaries Γ_1 and Γ_2 can then be constructed, using (17) and (20). It is noticed that the unknown variables associated with (17) and (20) are now discrete.

B. Fields in Free Space III

Using the Green's theorem and the radiation condition, one has the expression for the wave field $\phi = E_y$ or $\omega\mu_0 H_z$ in $(X_0 \le x < \infty, -\infty < z < \infty)$

$$\phi(x, z) = -\int_{-\infty}^{\infty} dz' \left(G \frac{\partial \phi}{\partial x'} - \phi \frac{\partial G}{\partial x'} \right) \Bigg| x' = X_0, \quad (x, z) \in III. \quad (22)$$

The two-dimensional Green's function G in free space is chosen as

$$G(z, z; x', z') = -\frac{j}{4} \left[H_1^{(2)}(k_1 r) + H_1^{(2)}(k_1 r_1) \right] \quad (23)$$

so that $\left. \frac{\partial G}{\partial x'} \right|_{x' = X_0}$ vanishes. Here $H_1^{(2)}$ is zero-order Hankel function of the second kind, and

$$r = \sqrt{(x' - x)^2 + (z' - z)^2}$$
$$r_1 = \sqrt{(2X_1 - x' - x)^2 + (z' - z)^2}. \quad (24)$$

We thus obtain

$$E_y(x, z) = -\int_{-\infty}^{\infty} dz' G(x - X_1, z - z') \cdot \frac{\partial}{\partial x'} E_y(X_1, z'), \quad (x, z) \in III \quad (25)$$

$$\omega\mu_1 H_z(x, z) = -j \int_{-\infty}^{\infty} dz' G(x - X_1, z - z') \cdot \frac{\partial^2}{\partial x'^2} E_y(X_1, z'), \quad (x, z) \in III \quad (26)$$

where $\omega_{\mu 0} H_z = j \frac{\partial E_y}{\partial x'}$ has been used in (26) and

$$G(x - x', z - z') = -\frac{j}{2} \cdot H_0^{(2)} \left(k_0 \sqrt{(x - x')^2 + (z - z')^2} \right). \quad (27)$$

The integrations in (25) and (26) are divided into three parts: those over $-\infty < z' \le 0$, those over $l \le z' < \infty$, and those over $0 \le z' \le l$. The first two parts are calculated by partially differentiating (10) with respect to x, and are functions of A_m and h_q^α as a result of (18) and (19). The field expression in (9) is substituted into the last part to make the integral depend on the nodal values ϕ_i of the elements adjacent to Γ_3. Finally, the exterior fields tangential to Γ_3 can be represented as

$$E_y(\Gamma_3^+) = \sum_m E_m A_m + \sum_\alpha \sum_q E_q^\alpha h_q^\alpha + \sum_i E_i \phi_i \quad (28)$$

$$\omega\mu_0 H_z(\Gamma_3^+) = \sum_m H_m A_m + \sum_\alpha \sum_q H_q^\alpha h_q^\alpha + \sum_i H_i \phi_i \quad (29)$$

where E's and H's are known functions of X_0 and z and are evaluated by the numerical methods.

IV. Numerical Procedure

By choosing the same basis functions for weighting fields $(E_y^a; H_x^a, H_z^a)$ and trial fields $(E_y; H_x, H_z)$, and using the representation (17), (20), (28), and (29) for exterior fields, we can solve the partial variational equation (8) by the finite element method along with the frontal solution technique [14]. Specifically, the expansion coefficients h_q^{I} and h_q^{II}, the nodal values ϕ_i along the boundaries Γ_1, Γ_2, and those of the elements adjacent to Γ_3 are arranged as the unknowns of the last element. Thus after the assembly and elimination process of the frontal solution technique, a matrix equation of the form

$$\bar{\bar{A}} \cdot \bar{\varphi} = \bar{s} \quad (30)$$

is finally obtained and solved by the Gaussian elimination process. Here $\bar{\bar{A}}$ is a known matrix, $\bar{s}$ is a known source vector due to the incident fields, and $\bar{\varphi}(= [\phi_i, h_q^{\mathrm{I}}, h_q^{\mathrm{II}}]^T)$ is a vector associated with the unknown coefficients.

After solving h_q^{I} and h_q^{II}, the reflection coefficients a_m and d_ρ may then be calculated from (18) and (19), respectively. The forward radiation field $E_y^R(r, \theta)$ is obtained by first extending the integration region of ρ (referred to (10)) to $(-\infty, \infty)$ and then utilizing the saddle-point method [15]:

$$|E_y^R(r, \theta)| \simeq \frac{\omega\mu_0}{\sqrt{k_0 r}} |d_\rho^{\mathrm{II}}|_{\rho = k_0 \sin\theta}, \quad k_0 r \gg 1, \ 0 \le \theta \le \frac{\pi}{2}. \quad (31)$$

Here (r, θ) are the polar coordinates of (x, z),

$$x = r \sin\theta, \ z = r \cos\theta. \quad (32)$$

V. Numerical Results

To test the validity of the approach, our results are compared with those of Gelin *et al.* [8], as shown in Fig. 3. When the normalized frequency $k_0 t$ becomes greater than 1.06, not only the dominant mode (a_1) but also the second-order mode (a_2) are excited and reflected back. The results show good agreement between the two methods. Other numerical checks of the present approach can also be found in other research on the discontinuity problem for two slab guides [13].

Several antenna (or discontinuity) structures for analysis are illustrated in Fig. 4, where either the structure parameters $(l/t, h/t)$ or the normalized frequency $k_0 t$ are considered as variables. We assume that all feeding slab waveguides are monomode, and that only the dominant mode with amplitude $A_1 = 1$ is incident upon the discontinuity structures.

Fig. 5 shows the reflection coefficient $|a_1|$ for the structures in Figs. 4(a)–4(e). The result for structure Fig. 4(a) is constant because the end is abruptly terminated and is independent of l/t. The reflection coefficients for the tapered structures (Figs. 4(b) and 4(c)) are less than that for the abrupt one in Fig. 4(a), and are decreased as the taper length is increased. The structures in Figs. 4(a)–4(c) have only one step junction, while the structures in Figs. 4(d) and 4(e) have two step ones. Reflected waves from the two step junctions interfere with each other, which causes oscillations in the

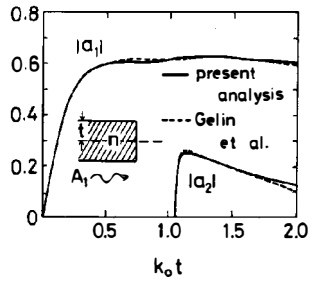

Fig. 3. Reflection coefficients of abruptly terminated planar dielectric structure excited by dominant guided mode. $n = 3.162$.

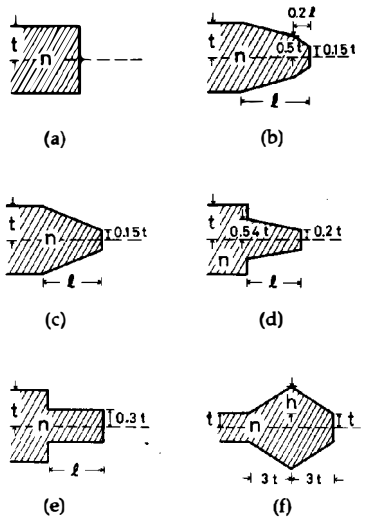

Fig. 4. Antenna structures for analysis.

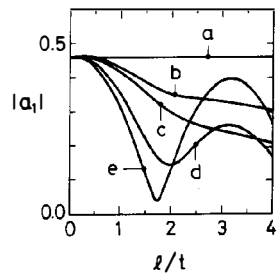

Fig. 5. Reflection coefficients of the structures in Fig. 4(a)-(e). $k_0 t = 0.8$, $n = 2.236$.

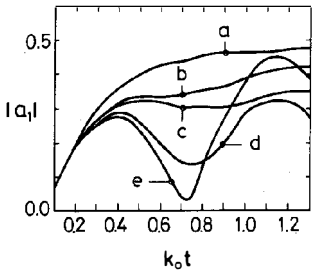

Fig. 6. Reflection coefficients of the structures in Fig. 4(a)-(e). $l/t = 2$, $n = 2.236$.

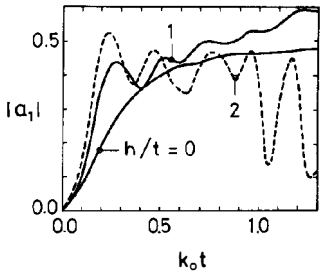

Fig. 7. Reflection coefficients of the structure in Fig. 4(f). $n = 2.236$.

reflection coefficient curves d and e in Fig. 5. The first dip of curve e happens at $l/t = 1.7$, which is somewhat apart from that ($l/t = 1.5$) of the effective dielectric constant (EDC) approximation [16], a result due to the excitation of higher order modes at the junction. The tapered configuration in Fig. 4(d) may weaken the interferences, and thus smooths out the corresponding reflection curve d in Fig. 5.

With respect to the same structures (Figs. 4(a)-4(e)), the frequency dependence of the reflection coefficients $|a_1|$ is plotted in Fig. 6, where the normalized lengths l/t are kept constant ($l/t = 2$). When the normalized frequency is low ($k_0 t < 0.2$), all the curves converge and approach zero because of the smallness of the waveguide and discontinuities. For $k_0 t > 0.4$, the reflection coefficients for structures (a) to (c) are nearly unchanged, and those for structures (d) and (e) show oscillations.

Shown in Fig. 7 are the reflection curves for the structure Fig. 4(f). Here, the normalized height h/t of the discontinuity is considered as a parameter. The structure for $h/t = 0$ corresponds to that of Fig. 4(a), namely an abruptly terminated end. The oscillatory phenomenon of the curves for $h/t = 1$ and 2 may be interpreted due to the interferences between the waves reflected from the positive-going (left) and negative-going (right) tapers. As suggested by the EDC approximation, when the wave is incident from a thick waveguide into a thin waveguide, the reflected wave is in-phase with the incident wave; otherwise, it is out-of-phase. Consequently the reflected waves are out-of-phase with the incident waves in the positive-going taper, and are in-phase in the negative-going taper. This suggests a possible mechanism for the curve oscillation.

Fig. 8 shows the normalized radiation patterns for the structure Fig. 4(e), where $k_0 t = 0.8$. The structure with $l/t = 0$ corresponds to the abruptly terminated end, and that with $l/t = 1.7$ corresponds to the one which has a minimum reflected power (Fig. 5). The directive gain and power gain are 5.50 and 4.52 dB for the former ($l/t = 0$), and are 5.77 and 5.77 dB for the latter ($l/t = 1.7$). Being similar in radiation patterns, the directive gains for both structures are approximately the same. Due to impedance matching, the power gain for $l/t = 1.7$ is 1.25 dB higher than that for the abruptly terminated end ($l/t = 0$), which means that better radiation efficiency can be achieved by the former structure.

Shown in Fig. 9 are the normalized radiation patterns for the structure Fig. 4(f), where the frequency ($k_0 t = 0.25$) is chosen so that the structure with $h/t = 2$ has a maximum reflected power. Although the half-power beamwidth of the

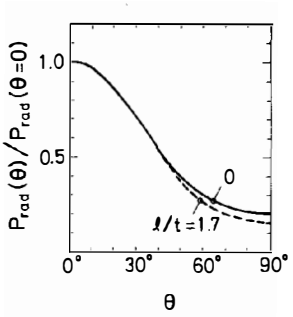

Fig. 8. Normalized radiation patterns of the structure in Fig. 4(e). $k_0 t = 0.8$, $n = 2.236$.

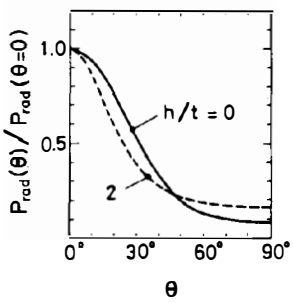

Fig. 9. Normalized radiation patterns of the structure in Fig. 4(f). $k_0 t = 0.25$, $n = 2.236$.

structure with $h/t = 2$ is less than that of the structure with $h/t = 0$, the directive gain (= 6.55 dB) of the former is somewhat smaller than that (= 6.85 dB) of the latter. This means that more radiated power is backward scattered in the structure of $h/t = 2$. In addition, the power gain for $h/t = 2$ (5.15 dB) is lower than that for $h/t = 0$ (6.60 dB) due to the higher reflectivity of the structure ($h/t = 2$).

VI. Conclusion

Radiation and scattering characteristics of several planar dielectric antenna structures have been examined, using the partial variational approach together with the finite element method. In this study, a hybrid exterior field representation has been proposed to tackle the radiation and boundary conditions. In particular, the reflection coefficients, the radiation patterns, and the gains of the antenna structures in Fig. 4 have been analyzed by varying the structure parameters (l/t,h/t) as well as the normalized frequency $k_0 t$. By following the similar approach, more arbitrarily shaped planar dielectric antennas with TE- or TM-mode excitation can be analyzed.

References

[1] C. M. Angulo, "Diffraction of surface waves by a semi-infinite dielectric slab," *IRE Trans. Antennas Propagat.*, vol. AP-5, pp. 100-109, Jan. 1957.

[2] J. K. Butler and J. Zoroofchi, "Radiation fields of GaAs-(AlGa)As injection lasers," *IEEE J. Quantum Electron.*, vol. QE-10, pp. 809-815, Oct. 1974.

[3] T. Ikegami, "Reflectivity of mode at facet and oscillation mode in double-heterostructure injection lasers," *IEEE J. Quantum Electron.*, vol. QE-8, pp. 470-476, June 1972.

[4] F. K. Reinhart, I. Hayashi, and M. B. Panish, "Mode reflectivity and waveguide properties of double-heterostructure injection lasers," *J. Appl. Phys.*, vol. 42, no. 11, pp. 4466-4479, Oct. 1971.

[5] G. A. Hockman, "Radiation from a solid-state laser," *Electron. Lett.*, vol. 9, pp. 389-391, 1973.

[6] L. Lewin, "Obliquity-factor for radiation from a solid-state laser," *Electron. Lett.*, vol. 10, pp. 134-135, 1974.

[7] ——, "A method for the calculation of the radiation- pattern and mode-conversion properties of a solid-state heterojunction laser," *IEEE Trans. Microwave Theory Tech.*, vol. MMT-23, pp. 576-585, July 1975.

[8] P. Gelin, M. Petenzi, and J. Citerne, "Rigorous analysis of the scattering of surface waves in an abruptly ended slab dielectric waveguide," *IEEE Trans. Microwave Theory Tech.*, vol. MTT-29, pp. 107-114, Feb. 1981.

[9] T. E. Rozzi and G. H. In'tVeld, "Variational treatment of the diffraction at the facet of d.h. lasers and of dielectric millimeter wave antennas," *IEEE Trans. Microwave Theory Tech.*, vol. MTT-28, pp. 61-73, Feb. 1980.

[10] E. Nishimura, N. Morita, and N. Kumagai, "Scattering of guided modes caused by an arbitrarily shaped broken end in a dielectric slab waveguide," *IEEE Trans. Microwave Theory Tech.*, vol. MTT-31, pp. 923-930, Nov. 1983.

[11] C. N. Capsalis, J. G. Fikioris, and N. K. Uzunoglu, "Scattering from an abruptly terminated dielectric-slab waveguide," *J. Lightwave Technol.*, vol. LT-3, pp. 408-415, Apr. 1985.

[12] S.-J. Chung and C. H. Chen, "Partial variational principle for electromagnetic field problems: theory and applications," *IEEE Trans. Microwave Theory Tech.*, vol. 36, pp. 473-479, Mar. 1988.

[13] ——, "A partial variational approach for arbitrary discontinuities in planar dielectric waveguides," *IEEE Trans. Microwave Theory Tech.*, vol. 37, pp. 208-214, Jan. 1989.

[14] E. Hinton and D. R. J. Owen, *Finite Element Programming*. New York: Academic, 1977.

[15] T. E. Rozzi, "Rigorous analysis of the step discontinuity in a planar dielectric waveguide," *IEEE Trans. Microwave Theory Tech.*, vol. MTT-26, pp. 738-746, Oct. 1978.

[16] T. E. Rozzi, T. Itoh, and L. Grun, "Two-dimensional analysis of the GaAs d.h. stripe-geometry laser," *Radio Sci*, vol. 12, no. 4, pp. 543-549, July-Aug. 1977.

Shyh-Jong Chung was born in Taipei, Taiwan, Republic of China, on January 18, 1962. He received the B.S.E.E. degree in 1984, and the Ph.D. degree in 1988, both from National Taiwan University, Taipei, Taiwan.

In 1988, he joined the Department of Communication Engineering, National Chiao Tung University, Hsinchu, Taiwan, ROC. During the time from 1989 to 1991, he was in the Army of ROC. His areas of interest include waveguide discontinuity problems, integrated optics, wave propagation, and numerical techniques in electromagnetics.

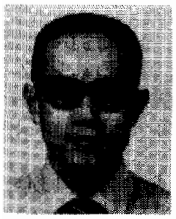

Chun Hsiung Chen (SM'88) was born in Taipei, Taiwan, Republic of China, on March 7, 1937. He received the B.S.E.E. degree from National Taiwan University, Taipei, Taiwan, in 1960, the M.S.E.E. degree from National Chiao Tung University, Hsinchu, Taiwan, in 1962, and the Ph.D. degree in electrical engineering from National Taiwan University in 1972.

In 1963, he joined the faculty of the Department of Electrical Engineering, National Taiwan University, where he is now a Professor. From 1982 to 1985 he was Chairman of the department. In 1974 he was a Visiting Researcher for one year with the Department of Electrical Engineering and Computer Sciences, University of California, Berkeley. From 1986 to 1987, he was a Visiting Professor with the Department of Electrical Engineering, University of Houston, TX. During June and July 1989, he visited the Microwave Department, Technical University of Munich, Germany. His areas of interest include antenna and waveguide analysis, propagation and scattering of waves, and numerical techniques in electromagnetics.